Available online at www.sciencedirect.com

ScienceDirect

Procedia Structural Integrity 64 (2024) 392–399

Structural Integrity Procedia

www.elsevier.com/locate/procedia

SMAR 2024 – 7th International Conference on Smart Monitoring, Assessment and Rehabilitation of Civil Structures

Experimental study on semi-cyclic loading effects on Fe-SMA reinforced concrete structures

Antoni Mir[a], Sandra del Río-Bonnín[a], Carlos Ribas[a], Joaquín G. Ruiz-Pinilla[a], Antoni Cladera[a]*

[a]*Universitat de les Illes Balears, Ctra.Valldemossa, km 7.5, Palma (Illes Balears), 07122, Spain*

Abstract

Concrete structures often face unforeseen challenges, whether from degradation or unexpected actions, requiring innovative strengthening techniques to extend their lifespan. In the last decade, shape-memory alloys (SMAs) have gained significant attention in structural engineering owing to their unique ability to recover from deformation, attributed to the shape-memory effect (SME). When constrained, SMAs can act as prestressing reinforcement, generating recovery stresses upon activation (heating and cooling). Among the various SMAs, iron-based SMAs (Fe-SMAs) have demonstrated exceptional potential for structural strengthening. Nonetheless, recent research has shown that Fe-SMA rebars may experience losses in recovery stresses when subjected to semi-cyclic loading.

This paper presents the results of an experimental campaign focused on assessing the impact of semi-cyclic loading on concrete beams reinforced with Fe-SMA bars. The reinforced concrete test specimens were subjected to semi-cyclic loads before and/or after the activation of the Fe-SMA bars. The preliminary findings show the effectiveness of Fe-SMA rebars as prestressing reinforcements despite semi-cyclic loads, especially when considering multiple activations throughout a structure's lifecycle. Therefore, this research provides valuable insights into enhancing the durability and safety of existing reinforced concrete structures by using Fe-SMAs.

Keywords: Iron-based Shape Memory Alloys; Activation; Prestressing reinforcements; Precamber; Semi-cyclic loading

* Antoni Cladera. Tel.: 971 171378; fax: +34-971 17 3426.
E-mail address: antoni.cladera@uib.es

10.1016/j.prostr.2024.09.273

1. Introduction

Existing concrete structures are continuously exposed to unforeseen challenges and degradation that compromise their service lives. To ensure the safety and functionality of these structures, retrofitting and structural rehabilitation are essential to extend their lifespan. Additionally, with the growing impact of climate change, there is a need to make the construction sector more sustainable and contribute to the development of a low-emissions sector. It is therefore important, given the high consumption of energy and raw materials that demolition and new construction involve, to commit to strengthening techniques that lead to the target of net-zero emissions (International Energy Agency, 2020; Li et al., 2023).

To address these challenges, research in the last decades has focused on new and sustainable reinforcement techniques. In this context, the use of Shape Memory Alloys (SMAs) has gained significant attention in the field of structural engineering due to their unique ability to return to their original form (after being deformed) upon activation (heating and subsequent cooling)(Izadi et al., 2018). This property, known as the shape memory effect (SME), makes SMAs attractive for use as prestressing reinforcement, currently being mainly developed at Swiss Federal Laboratories for Materials Science and Technology (EMPA) (Schranz, 2021; Schranz et al., 2019, 2021). Among the different types of SMAs, Iron-Based Shape Memory Alloys have shown exceptional potential for structural strengthening, with the added benefit of cost reduction (Mas et al., 2016).

The application of Fe-SMA reinforcement for prestressing concrete structures requires two main actions. First, a prestraining of the material between 2 and 4% to induce the forward martensitic transformation, which generates martensite at the atomic level, followed by a complete unloading. Second, an activation of the material after being embedded in concrete or externally bonded to the concrete structure. Upon heating the SMA, the reverse transformation is induced, generating austenite, and the Fe-SMA attempts to return to its original form (before prestraining). However, if the Fe-SMA is correctly fixed to or embedded in the concrete structure, deformation will be impeded, and recovery stresses induced in the material will lead to a prestressing effect in the structure (Ruiz-Pinilla et al., 2020a, 2020b).

Most of the strengthening techniques employed are passive strengthening techniques, meaning the material does not start to structurally contribute until a certain level of deformation is reached. In contrast, SMAs can be used as active reinforcement due to the SME. Consequently, the reinforcement becomes fully operational immediately upon its placement and activation, introducing prestressing that ensures the material contributes to the structure instantly (Cladera et al., 2014). Nonetheless, there are still unknowns concerning the SMAs capacity to maintain prestressing over time, particularly under the influence of semi-cyclic loads as shown by Schranz, Czaderski, et al. (2019), typical in the daily use of structures.

This paper reports the outcomes of an experimental campaign aimed at evaluating the effects of semi-cyclic loading on concrete elements reinforced with Fe-SMA bars. The specimens were reinforced with 16 mm ribbed Fe-SMA bar, provided by the Swiss company *re-fer AG* (https://www.re-fer.eu/), and exposed to semi-cyclic loading either before and/or after the activation of the Fe-SMA rebars. These tests aimed to assess the effectiveness of the prestressing induced by the Fe-SMA when subjected to semi-cyclic loads and a second activation throughout the lifespan of the structure.

2. Description of the experimental campaign

2.1. Manufacturing process

The beam specimens dimensions were 100x200x3550 mm with a clear span of 1950 mm. The two beams were longitudinally reinforced with one ϕ10 mm standard B500SD rebar (f_y = 534 MPa and f_u = 637 MPa) placed at the tensile chord during the activation (top part of the cross section) but at the compression chord during the load test (bottom part of the cross-section, as the beams were turned up-side down after the construction and initial activation). The tensile reinforcement of the beams consisted of one ϕ16 mm Fe-SMA bar, already prestrained to 4% by the supplier, with a cross-section (A_{SMA}) equal to 211 mm^2. The ultimate strength (f_u) and strain (ε_u) of the as-provided Fe-SMA bars were 786 MPa and 25%, respectively. The mean 0.2% proof stress ($f_{0.2}$), obtained by the offset method, was 491 MPa. The modulus of elasticity of the Fe-SMA bar (E_{SMA}), calculated between 150 and 250

MPa, was 118 GPa. For the activated Fe-SMA bars, f_u and ε_u were equal to 782 MPa and 31%, respectively. The $f_{0.2}$ was 489 MPa, and E_{SMA} was 50 GPa (measured between 350 MPa and 450 MPa).

The specimens were manufactured in two phases. The first phase included the arrangement of the longitudinal B500SD and ϕ16 mm Fe-SMA reinforcement, as indicated in Figure 1. The Fe-SMA bars were partially left unconcreted (corresponding to the test zone defined in Figure 1) to facilitate the activation of the Fe-SMA bars with an industrial blowtorch. The second phase, once the Fe-SMA was activated, included the casting of the concrete cover of the test zone.

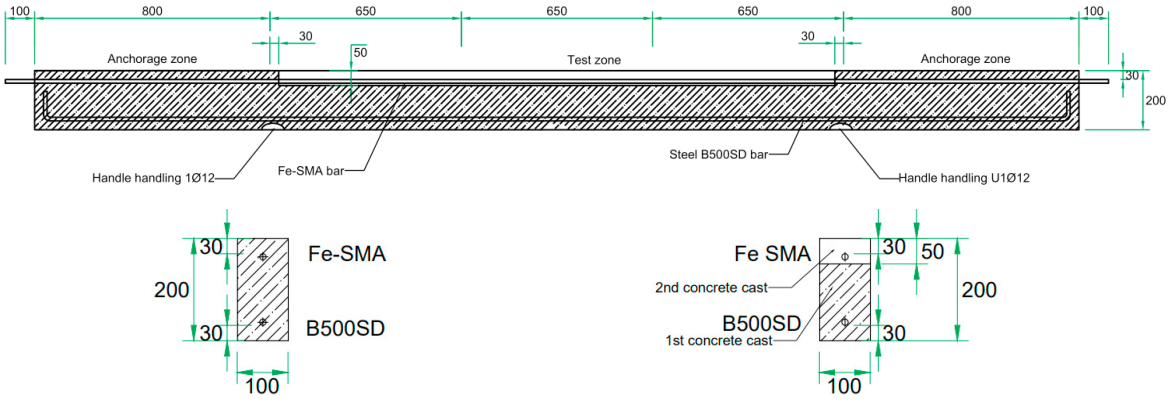

Figure 1. Geometrical characteristics of the specimens during manufacturing and first activation. Dimensions in mm

2.2. Test setup and instrumentation

The test setup of the experimental campaign could be divided into 3 stages. The 1st included an initial activation to 250ºC of the Fe-SMA bar with an industrial blowtorch (Figure 2a). Upon activation, as the Fe-SMA bar was previously prestrained, it attempted to return to its initial form, generating recovery stresses since the deformation of the bar was impeded by the anchorage of the Fe-SMA bar in the concrete (see anchorage zone in Figure 1). The recovery stresses generated within the bar lead to a prestressing effect on the structure, resulting in a precamber. Three high-resolution cameras were placed across the beam length to monitor the test (Figure 2b)

(a)

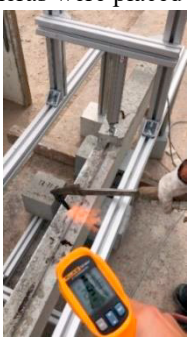

(b)

Figure 2. First activation procedure: (a) activation with an industrial blowtorch; (b) activation setup.

For comparison purposes, one specimen underwent initial activation while the other did not. Hence, the chosen nomenclature for designating the beams was S1-ϕ16-CP for the specimen that was not initially activated and subjected to semi-cyclical loads in its as-provided form ("*P*" from as Provided). In contrast, specimen S2-ϕ16-CA underwent initial activation ("*A*" from Activated) before the application of the semi-cyclical loads, as detailed in Table 1. These beams are part of a broader experimental campaign involving the manufacture and testing of 8 specimens designed to assess the impact of reinforcing the beams with 11-mm and 16-mm Fe-SMA bars.

Table 1. Designation and main characteristics of the tested beams.

Beam designation	b [mm]	h [mm]	Fe-SMA rebar diameter (ϕ) [mm]	A_{SMA} [mm^2]	E_{SMA}[GPa]*	First activation
S1- ϕ16-CP	100	200	16	211	118	No
S2- ϕ16-CA	100	200	16	211	50	Yes

* Measured between 150 and 250 MPa for the as provided ample and between 350 and 450 MPa for the activated sample.

The second stage consists of the application of semi-cyclic loads to both specimens with Figure 3 layout. Beams were subjected to load cycles (without sign inversion) under force control. Seven incremental load steps were applied, starting with a preload of 0,5 kN and increasing by 5 kN each time, reaching a maximum load of 35,5 kN. For each load step, the semi-cycles were repeated three times. Consequently, after the preload, the test began with three semi-cyclic loads at 5,5 kN (loading to 5,5 kN and unloading to 0,5 kN), followed by three semi-cyclic loads at 10,5 kN (loading to 10,5 kN and unloading to 0,5 kN), then 15,5 kN, and so forth, until reaching 35,5 kN.

The load level achieved did not attempt to reproduce any realistic loading scenario. The aim of this experimental campaign was to assess the behavior of concrete elements reinforced with Fe-SMA bars under semi-cyclic loads. The maximum load level was chosen based on the predicted shear strength of the beam specimens, which was 41 kN, to ensure the beams were loaded to a sufficiently lower level to prevent shear failure.

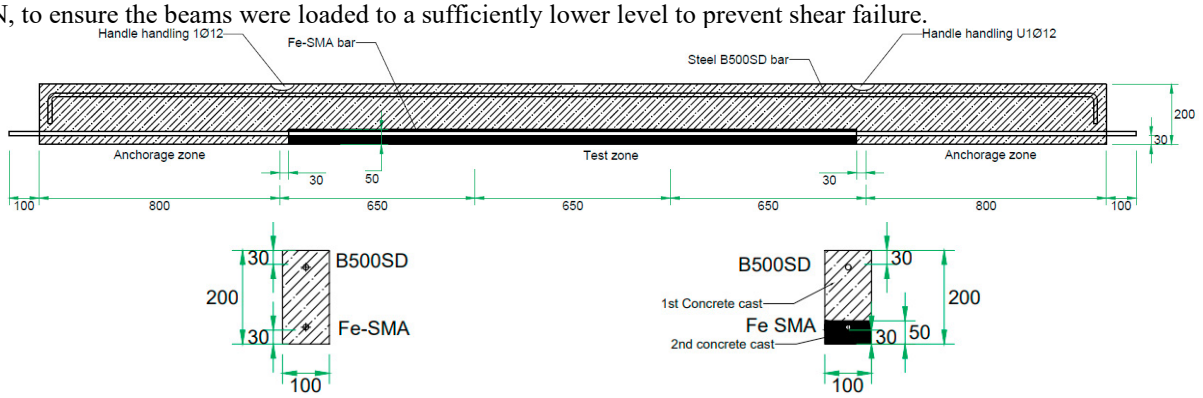

Figure 3. Geometrical characteristics of the specimens during semi-cyclical load test and 2nd activation. Dimensions in mm.

The third stage of the tests involved the activation of the Fe-SMA bar by applying an electric current using a power supply (Figure 4a and Figure 4b). The bar was heated to 160ºC (Figure 4c), and subsequently cooled to room temperature. This activation provided insights on Fe-SMA behavior after being subjected to a second activation (in the case of specimen S2- ϕ16-CA) and semi-cyclic loading.

(a) (b) (c)

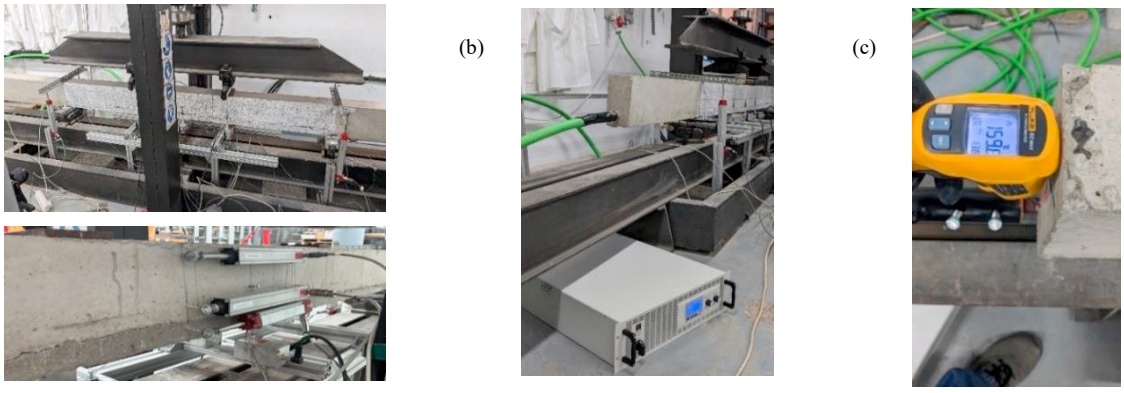

Figure 4. (a) Test setup and instrumentation; (b) Connection of the power supply to the Fe-SMA bars; (c) Activation of Fe-SMA bar to 160 ºC.

During the tests, the deflection and support displacements, compressions, and tensile deformations of the mid-span section were monitored by 6 Linear Variable Differential Transformers (LVDTs) and 4 Encoders (ECs) (Figure 3a). The strains at the Fe-SMA bar were monitored by 3 Linear Strain Gauges (LSGs) and 3 Linear High-Temperature Strain Gauges (LHTSGs). One LSG was attached to the B500SD bar.

3. Results and discussions

3.1. First activation procedure

Figure 5 presents the evolution of deflection at the mid-span section. At the end of the test, a precamber (δ) of 7.25 mm was generated through the heating and subsequent cooling of the Fe-SMA bar. This process leads to the prestressing of the structure, resulting in an estimated prestressing stress in the Fe-SMA bar (f_p) equal to 255 MPa for this specimen. This stress was calculated from the value of the precamber assuming cracked section and linear stress-strain behavior of the materials. In the characterization campaign, the mean recovery stress value obtained from activating a 16-mm Fe-SMA bar to 250ºC was 316 MPa, which is slightly higher than the one generated in the 1st activation procedure.

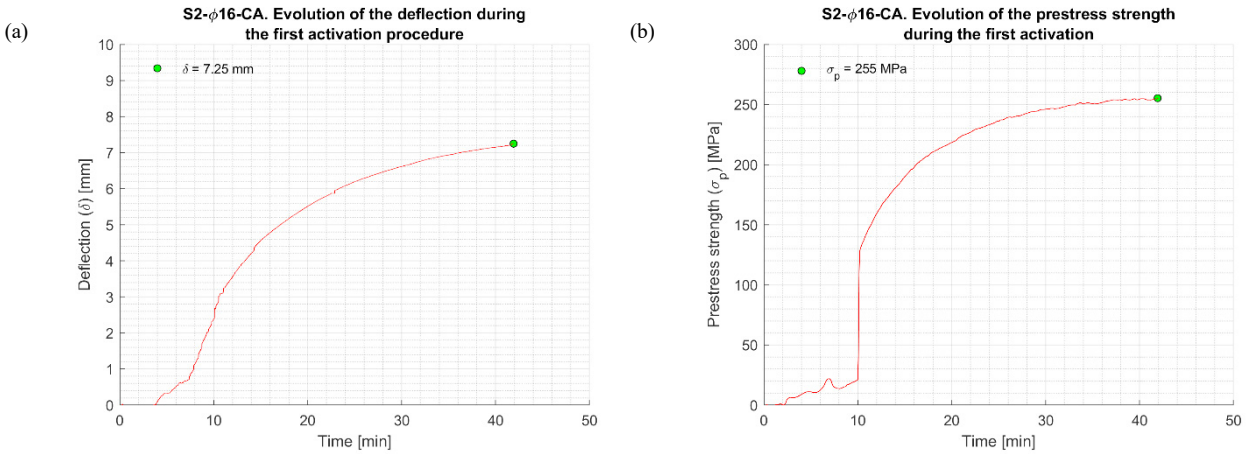

Figure 5. (a) Precamber and (b) estimated prestress strength generated at specimen S2- ϕ16-CA during the first activation procedure.

3.2. Semi-cyclic loading tests

In Figure 6, two scenarios are compared regarding the evolution of deflection under semi-cyclic load for specimens S2-ϕ16-CA and S1-ϕ16-CP. The left figure represents data without considering the previously determined precamber of specimen S2-ϕ16-CA, while the right figure incorporates this precamber. It is observed that specimen S2-ϕ16-CA displays a higher increment of deflection values compared to beam S1-ϕ16-CP under the same applied load, indicating a less rigid response. This observation can be attributed to two primary reasons: 1) a decrease in the modulus of elasticity of the Fe-SMA bar after activation, as indicated by the characterization results of the Fe-SMA; 2) during activation of S2-ϕ16-CA cracks opened in the opposite concrete parament decreasing the stiffness of the beam because the bending moment had to close them when the semi-cyclic load was applied. However, in Figure 6b, is seen that the total deflection is lower in the specimen with activated Fe-SMA bar when the initial deflection is considered. Moreover, when unloading the specimens after the application of semi-cyclical loads, specimen S2-ϕ16-CA did not completely lose the precamber acquired through the initial activation. The results in both specimens demonstrate the effectiveness of prestressing by activating a Fe-SMA bar.

(a) (b)

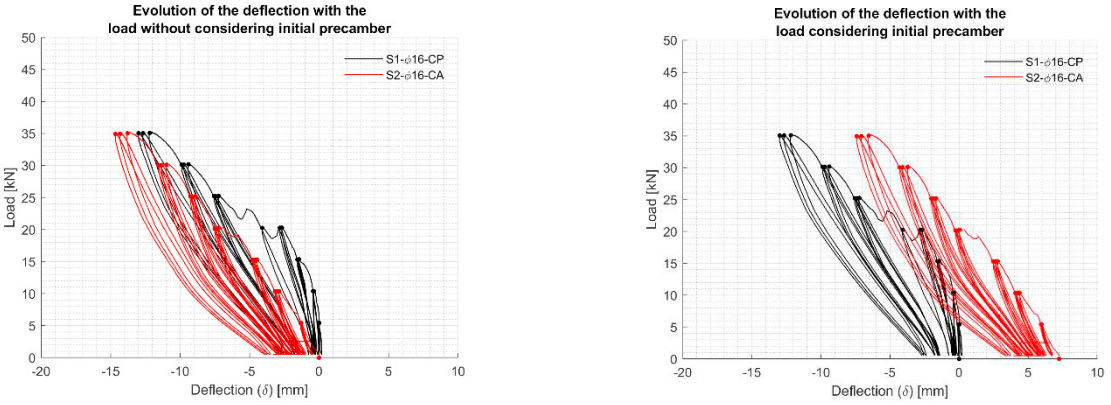

Figure 6. Deflection vs. load. (a) Without considering initial precamber; (b) Considering initial precamber of specimen S2-ϕ16-CA.

3.3. Activation after semi-cyclic loading tests

A new activation procedure was conducted subsequent to the semi-cyclical loading test, this time for both specimens. This activation was the second activation for specimen S2-ϕ16-CA and the first activation for S1-ϕ16-CP (in any case, it will be referred as "2nd activation" in the next sections for both cases). The purpose of this activation was to assess the prestressing capacity of the Fe-SMA after being subjected to semi-cyclic loads.

The bars were heated to 160ºC and then allowed to cool to ambient temperature. On this occasion, activation was achieved by using a power supply connected to the protruding ends of the bars, due to the direct inaccessibility of the Fe-SMA (Figure 3). Figure 7 compares the evolution of deflection with temperature, excluding the initial precamber of specimen S2-ϕ16-CA (Figure 7a) and including it (Figure 7b).

(a) (b)

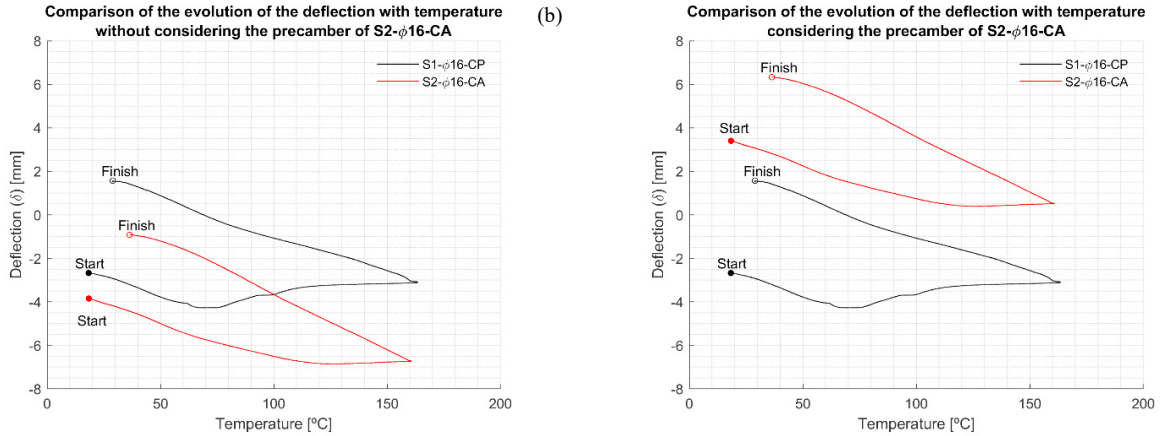

Figure 7. Deflection vs. temperature for 2nd activation. (a)Without considering initial precamber; (b)Considering initial precamber of S2-ϕ16-CA.

Both the Figure 7 and Table 2 demonstrate that specimen S1-ϕ16-CP not only achieved a complete recovery from the deflection caused by the application of semi-cyclical loads but also improved upon its initial state, concluding the 2nd activation with a precamber of 1.58 mm.

Upon the 2nd activation of specimen S2-ϕ16-CA, the deflection induced by the semi-cyclical test was nearly counteracted, ending the test 0.918 mm below its initial state before the semi-cyclical loading test, which was 7.25 mm.

The prestressing stress (f_p) induced by the 2nd activation was 221 MPa for specimen S1-ϕ16-CP. In the case of specimen S2-ϕ16-CA, the increase in prestressing stress due to the 2nd activation was equal to 115 MPa (estimated from the deflection measured during the 2nd activation).

Table 2. Deflections before and after the semi-cyclical test and after activation. Positive values are referred to precamber.

Specimen	Initial precamber before semi-cyclical test [mm]	Residual deflection after semi-cyclical test (mm)	Final precamber after 2nd activation (mm)	Precamber generated due to the 2nd activation (mm)
S1- ϕ16-CP	0	-2.70	1.57	4.27
S2- ϕ16-CA	7.25	3.37	6.33	2.96

Figure 8 depicts the evolution of deflection throughout all the performed tests. Specimen S2-ϕ16-CA was initially activated and a precamber was generated. Then, both specimens (S1-ϕ16-CP and S2-ϕ16-CA) were subjected to semi-cyclical loads and subsequently activated to 160ºC. The specimens overcame the effects of the semi-cyclic loads with the prestress effect induced by the activation of the Fe-SMA bar.

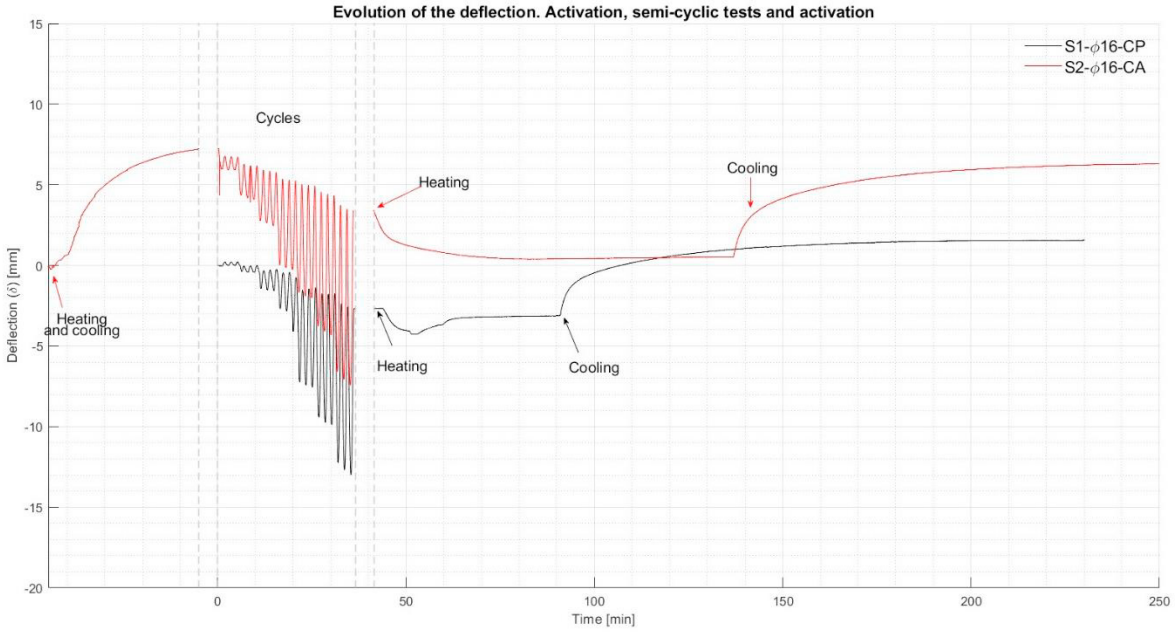

Figure 8. Evolution of the deflection during first activation, semi-cyclical tests and second activation for specimens S1- ϕ16-CP and S2- ϕ16-CA.

4. Conclusions

An experimental campaign was conducted to evaluate the capacity of Fe-SMA to maintain its prestressing ability after being subjected to semi-cyclic loads. The results of two beam specimens, which reflect the overall behaviour of the full experimental campaign, demonstrate the efficacy of using Fe-SMA bars as prestressing reinforcements even under semi-cyclical loads, especially when considering a possible second activation throughout a structure's lifecycle.

Fe-SMA bars showed the capacity to prestress the beams before and after the semi-cyclical loads, providing valuable insights into enhancing the safety of existing reinforced concrete structures through the use of Fe-SMA rebars for strengthening purposes.

This work has not established criteria for determining when a second activation might be appropriate in real structures. Future research by the authors will include a detailed analysis of the remaining six tested specimens, as well as the effects of multiple activations on the beam specimens. Additionally, a finite element method model will be developed to replicate the experimental results. This model will allow for a deeper understanding of the behaviour of concrete elements reinforced with Fe-SMA bars when subjected to semi-cyclic loads and will facilitate the study of these effects under more realistic loading scenarios.

5. Acknowledgements

This research was conducted as a part of projects CICLO, funded from Comunitat Autonòma de les Illes Balears through the Direcció General de Recerca, Innovació i Transformació Digital with funds from the Tourist Stay Tax Law (PDR2020/XX - ITS2017-006)., and PID2021-123701OB-C22 funded by MCIN/AEI/10.13039/501100011033 and by "ERDF A way of making Europe". Also acknowledge "SOIB/ Direcció General de Recerca, Innovació i Transformació Digital" and "European Union Next Generation EU" for the grant given to the first author.

6. References

Cladera, A., Weber, B., Leinenbach, C., Czaderski, C., Shahverdi, M., & Motavalli, M. (2014). Iron-based shape memory alloys for civil engineering structures: An overview. In *Construction and Building Materials* (Vol. 63, pp. 281–293). Elsevier Ltd. https://doi.org/10.1016/j.conbuildmat.2014.04.032

International Energy Agency. (2020). *Iron and Steel Technology Roadmap Towards more sustainable steelmaking Part of the Energy Technology Perspectives series*. www.iea.org/t&c/

Izadi, M. R., Ghafoori, E., Shahverdi, M., Motavalli, M., & Maalek, S. (2018). Development of an iron-based shape memory alloy (Fe-SMA) strengthening system for steel plates. *Engineering Structures*, *174*, 433–446. https://doi.org/10.1016/j.engstruct.2018.07.073

Li, L., Chatzi, E., Czaderski, C., & Ghafoori, E. (2023). Influence of activation temperature and prestress on behavior of Fe-SMA bonded joints. *Construction and Building Materials*, *409*. https://doi.org/10.1016/j.conbuildmat.2023.134070

Mas, B., Cladera, A., & Ribas, C. (2016). Fundamentos y aplicaciones piloto de las aleaciones con memoria de forma para su utilización en ingeniería estructural. *Hormigón y Acero*, *67*(280), 309–323. https://doi.org/10.1016/j.hya.2016.02.007

Ruiz-Pinilla, J. G., Montoya-Coronado, L. A., Ribas, C., & Cladera, A. (2020a). Finite element modeling of RC beams externally strengthened with iron-based shape memory alloy (Fe-SMA) strips, including analytical stress-strain curves for Fe-SMA. *Engineering Structures*, *223*. https://doi.org/10.1016/j.engstruct.2020.111152

Ruiz-Pinilla, J. G., Montoya-Coronado, L. A., Ribas, C., & Cladera, A. (2020b). Numerical modelling of reinforced concrete beams with a shear external strengthening using iron based shape memory allow. *Congreso de La Asociación Española de Ingeniería Estructural* .

Schranz, B. (2021). *Iron-based Shape Memory Alloy Reinforcement for Prestressed Strengthening of Concrete Structures* [ETH Zurich]. https://doi.org/10.3929/ethz-b-000499175

Schranz, B., Czaderski, C., Shahverdi, M., Michels, J., Vogel, T., & Motavalli, M. (2019). Ribbed iron-based shape memory alloy bars for pre-stressed strengthening applications. *IABSE Symposium 2019 Guimarães*.

Schranz, B., Michels, J., Czaderski, C., Motavalli, M., Vogel, T., & Shahverdi, M. (2021). Strengthening and prestressing of bridge decks with ribbed iron-based shape memory alloy bars. *Engineering Structures*, *241*. https://doi.org/10.1016/j.engstruct.2021.112467